

Supplementary Information

Structure-controllable superhydrophobic Cu meshes for effective separation of oils with different viscosities and aqueous pollutant purification

Stephen Boakye-Ansah¹, Yong Taek Lim¹, Ha-Jin Lee^{2}, and Won San Choi^{1*}*

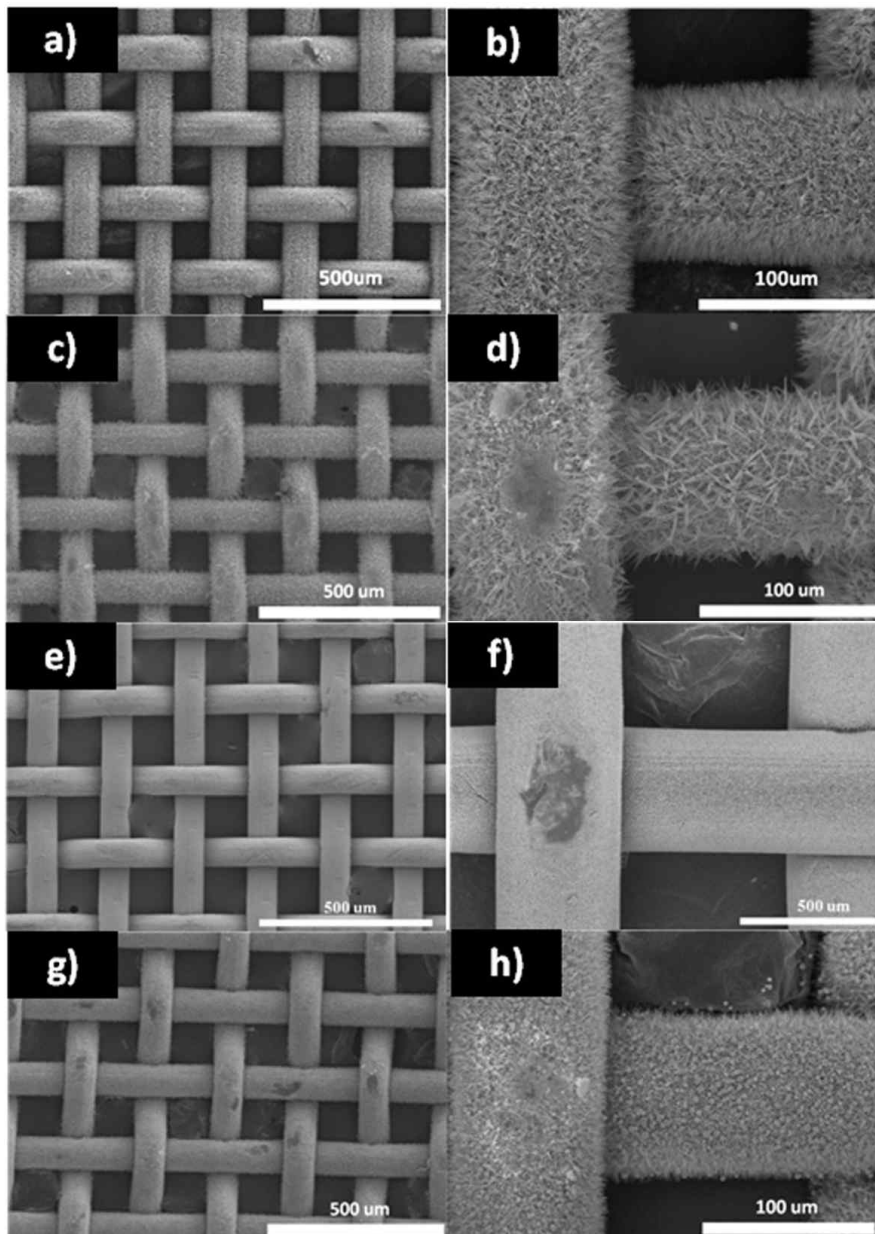


Figure S1. Low magnified SEM images of (a, b) NL, (c, d) HL, (e, f) AL, and (g, h) PNL meshes.

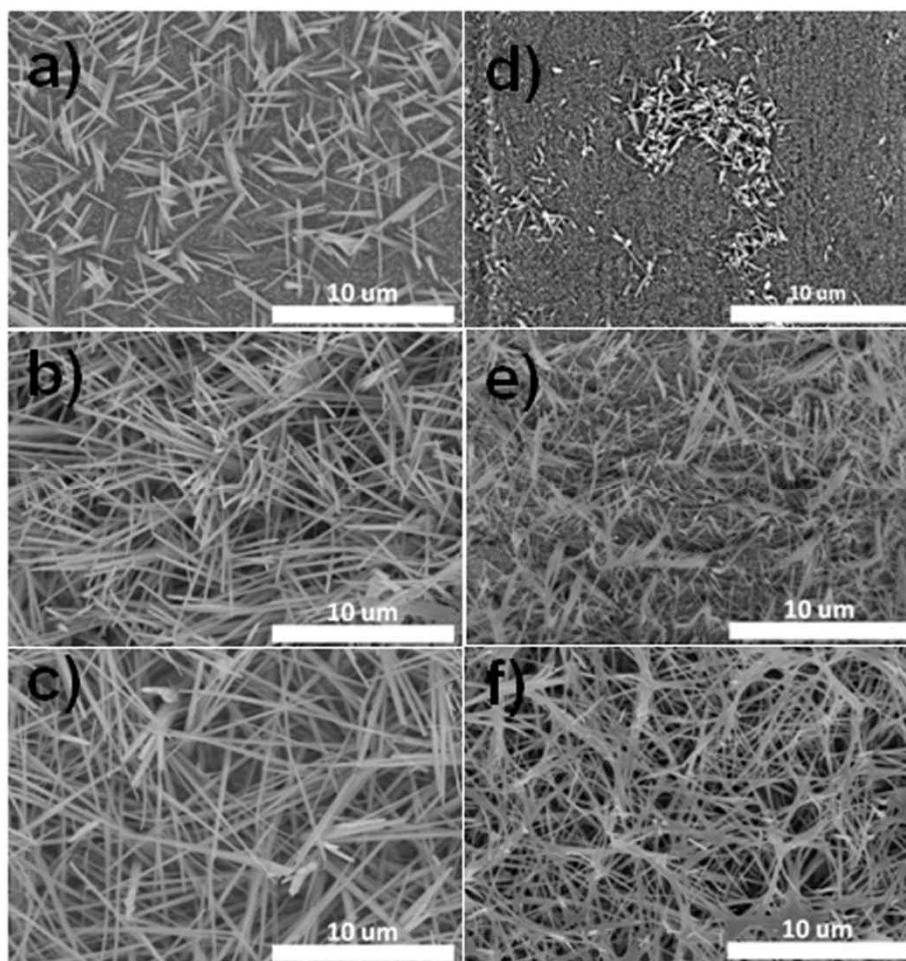


Figure S2. SEM images of the Cu mesh/CuO-Cu(OH)₂ as a function of reaction time and temperature. (a) (R.T., 10 min), (b) (R.T., 20 min), (c) (R.T., 30 min), (d) (40 °C, 10 min), (e) (40 °C, 20 min), and (f) (40 °C, 30 min).

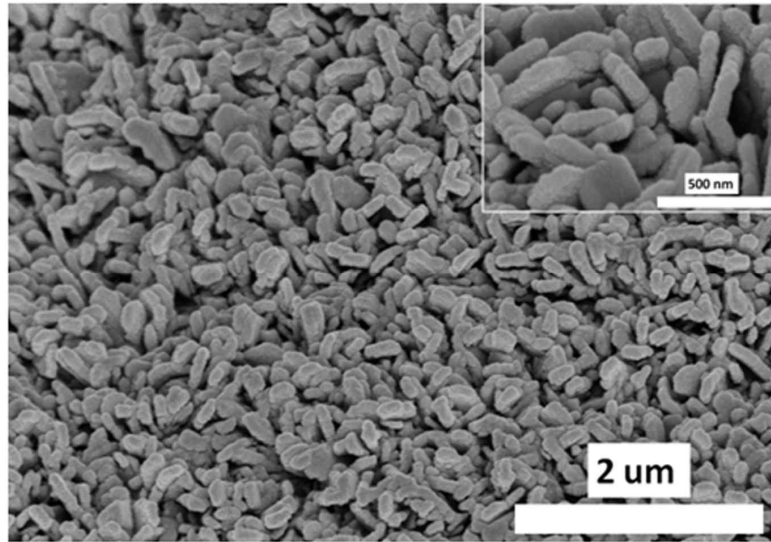


Figure S3. SEM images of the MPO-Cu mesh (Cu mesh/CuO-Cu(OH)₂) obtained after oxidation for 50 min.

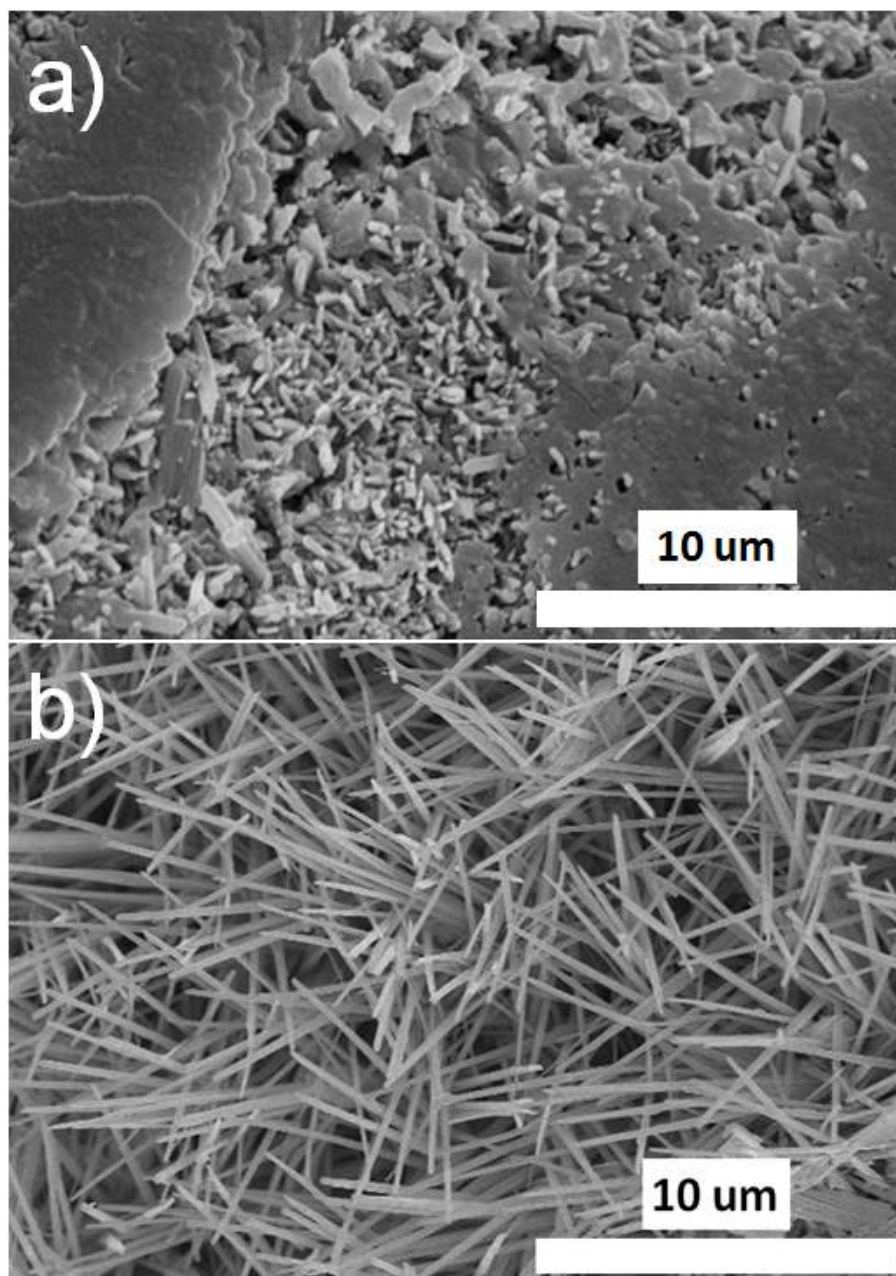


Figure S4. SEM images of the MPO-Cu mesh/PFTOS (a) before and (b) after annealing.

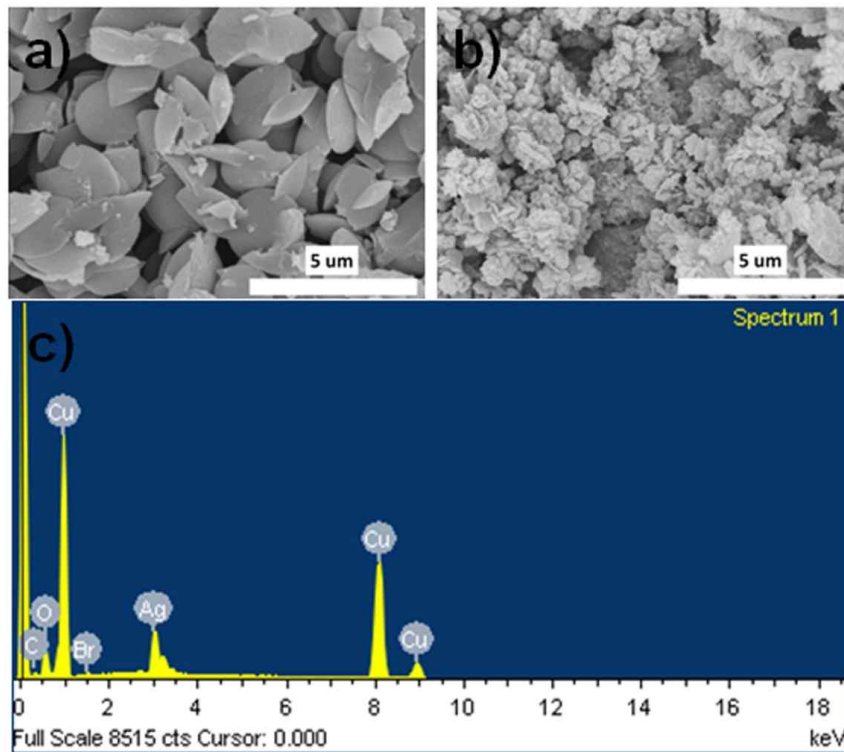


Figure S5. SEM images of (a) a MPO-Cu mesh/Pdop and (b) a MPO-Cu mesh/Pdop/Ag/AgBr. (c) EDX data of a MPO-Cu mesh/Pdop/Ag/AgBr.

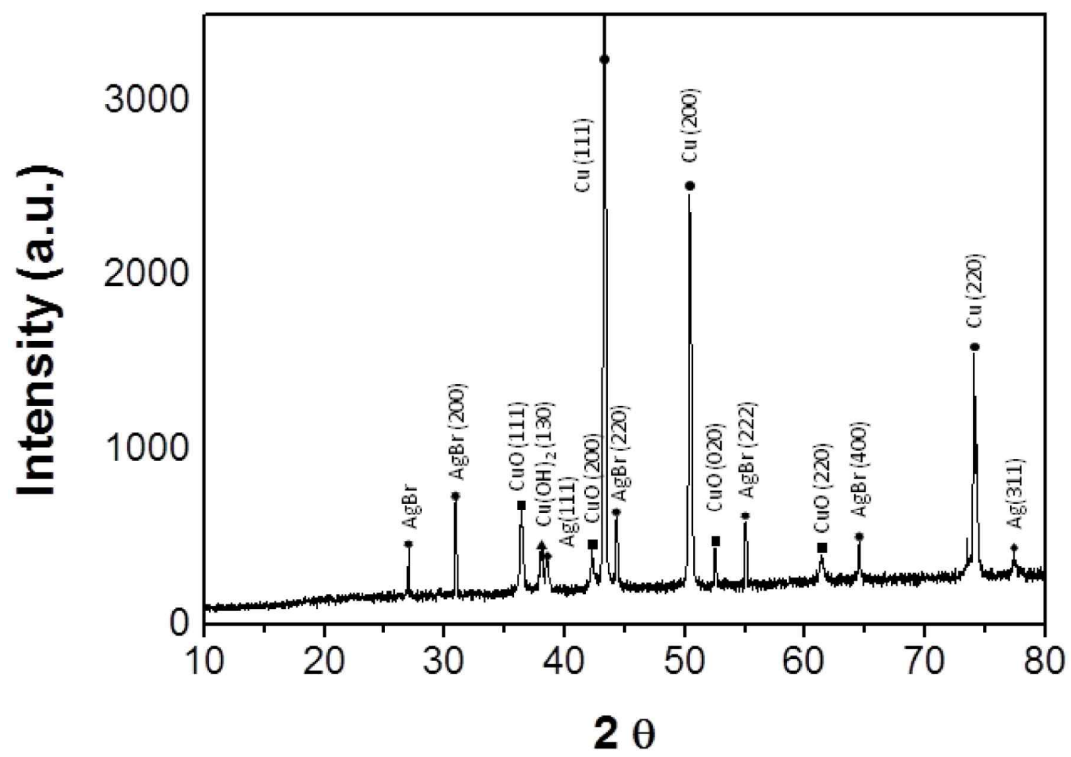


Figure S6. XRD pattern of a MPO-Cu mesh/Pdop/Ag/AgBr.

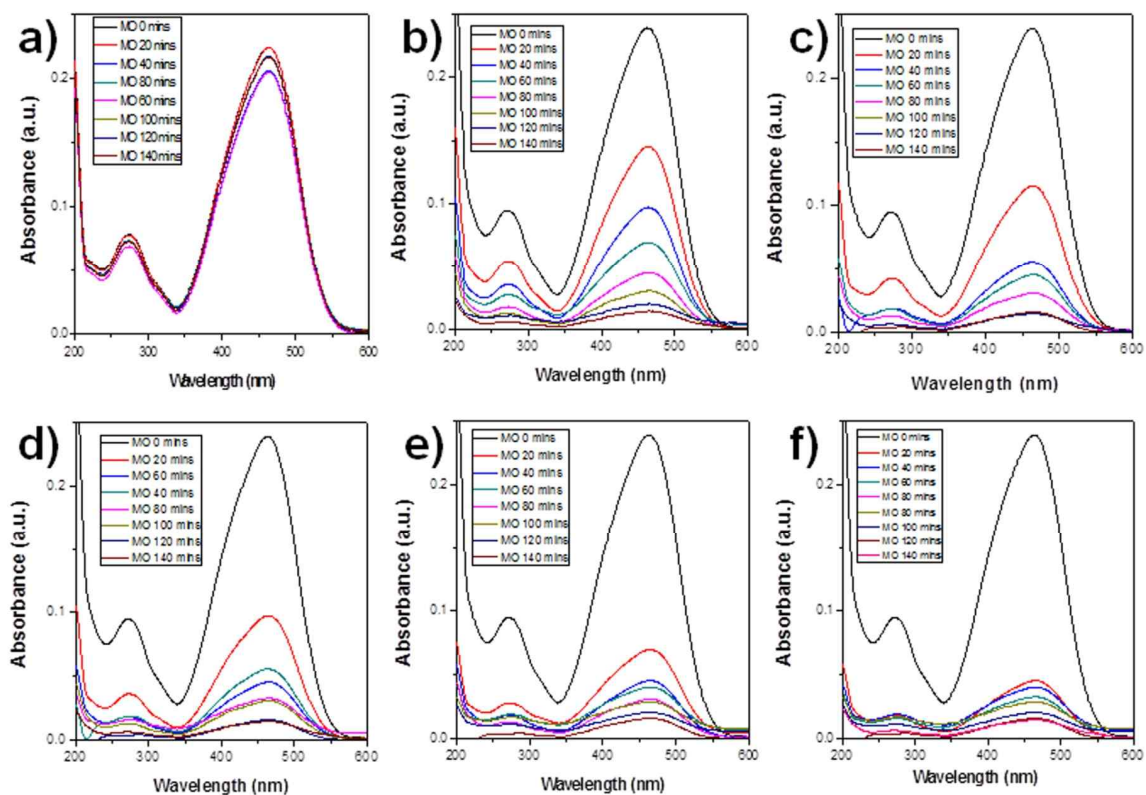


Figure S7. UV-vis spectra showing the decomposition of MO dyes catalysed by a photocatalytic mesh under visible-light irradiation: (a) without photocatalyst, (b) 1st cycle, (c) 2nd cycle, (d) 3rd cycle, (e) 4th cycle, and (f) 5th cycle.

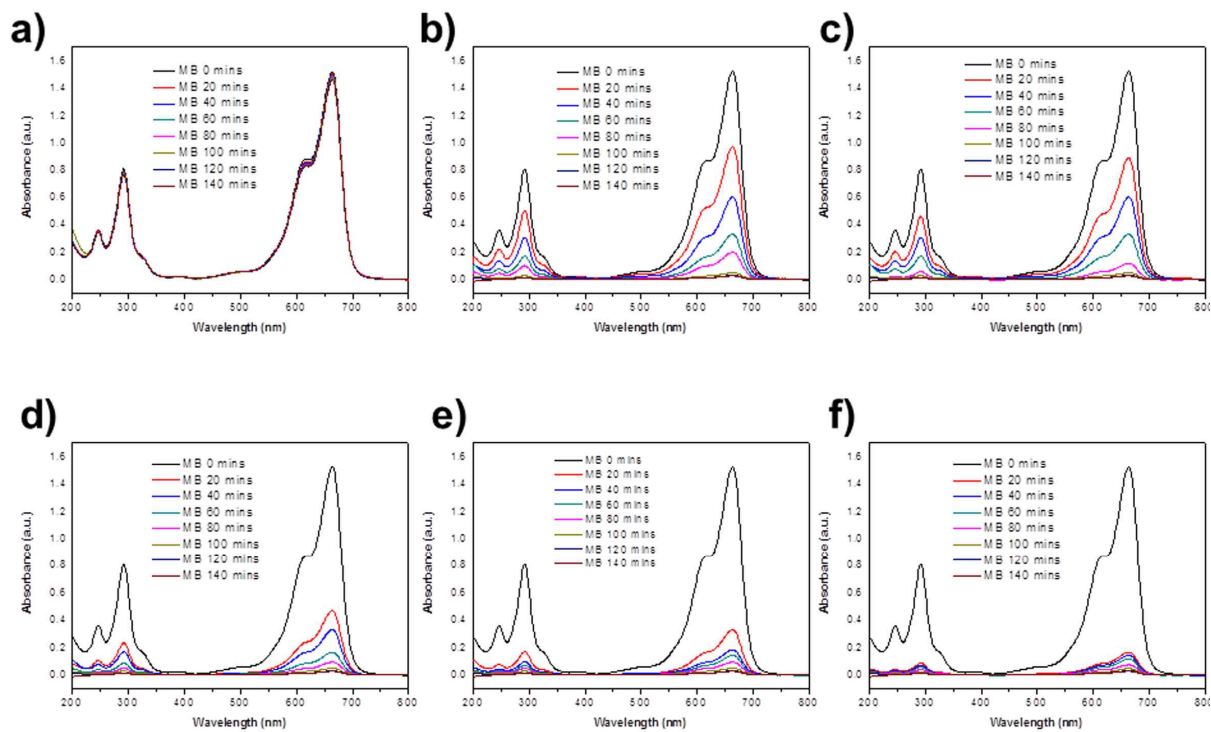


Figure S8. UV-vis spectra showing the decomposition of MB dyes catalysed by a photocatalytic mesh under visible-light irradiation: (a) without photocatalyst, (b) 1st cycle, (c) 2nd cycle, (d) 3rd cycle, (e) 4th cycle, and (f) 5th cycle.